AHM
Archives of Hand and Microsurgery

Original Article

pISSN 2586-3290 · eISSN 2586-3533
Arch Hand Microsurg 2021;26(3):152-160
https://doi.org/10.12790/ahm.21.0113

Received: July 19, 2021
Revised: August 1, 2021
Accepted: August 2, 2021

Corresponding author:
Jong-Pil Kim
Hand & Upper Extremity Center, Naeun Pil Hospital, 64 Mannam-ro, Dongnam-gu, Cheonan 31124, Korea
Tel: +82-41-550-3919
Fax: +82-41-550-3094
E-mail: kimjp7114@gmail.com
ORCID:
https://orcid.org/0000-0002-1913-9163

Topographic and Histologic Analysis of the Collateral Ligament Complex around the Elbow

Jong-Pil Kim[1,2], Ji-Kang Park[1,3], Joon-Young Yoo[1,2], Won-Jeong Shin[1], Jeong-Sang Kim[2], Young-IL Kim[2]

[1]Hand & Upper Extremity Center, Naeun Pil Hospital, Cheonan, Korea
[2]Department of Orthopedic Surgery, Dankook University College of Medicine, Cheonan, Korea
[3]Department of Orthopedic Surgery, Chungbuk National University College of Medicine, Cheungju, Korea

Purpose: The purpose of this study was to evaluate topographic anatomy of the footprints of key ligaments of the elbow and assess their relationships with bony parameters using micro-computed tomography (micro-CT). Additionally, the ratios of type I/III collagen at the medial collateral ligament (MCL) and lateral collateral ligament (LCL) of elbow were investigated.

Methods: Eleven cadaveric elbows attached by both the MCL and LCL were scanned using micro-CT and reconstructed three-dimensionally. Additionally, the ligaments were examined under polarized light microscopy to determine the histological characteristics of collagen patterns.

Results: Areas of footprints of the MCL and LCL attaching onto the humerus were 133.2±25.8 mm^2 and 128.3±23.2 mm^2, respectively. Footprint sizes of anterior and posterior bundles of the MCL in the proximal ulna and lateral ulnar collateral ligament (LUCL) attaching to the proximal ulna averaged to 109.9 mm^2, 89.2 mm^2, and 89.7 mm^2, respectively. There were a positive correlation between footprint size of the MCL and LUCL at the humeral side and a negative correlation between the footprint size of the MCL at humeral side and maximal diameter of the radial head. The collagen I/III ratio of the humeral attachment of the MCL was higher than distal attachment of the MCL.

Conclusion: This study provides a better understanding of the pathologies of the MCL and LCL complex of the elbow and their relationships with osseous anatomy and may assist the clinician with an anatomic reconstruction of the ligaments.

Keywords: Micro-computed tomography, Footprint, Collateral ligaments, Elbow, Collagen, Three-dimensional

INTRODUCTION

The elbow is an inherently stable joint complex, owing to its bony anatomy and soft tissue reinforcement [1]. Nevertheless, traumatic elbow injuries with accompanying avulsion of bone and resulting disruption of tendinous or ligamentous attachments occur with an incidence of 5.21/100,000 person-year [1]. Many unstable ligamentous injuries require surgical reconstruction of the elbow ligament [2-5].

The medial collateral ligament (MCL) complex of the elbow is divided into anterior, posterior, and transverse fiber bundles. Of these, the anterior bundle is much more closely packed than the posterior bundle [6,7] and is the major soft tissue restraint to valgus stress of the elbow [8]. The lateral collateral ligament (LCL) complex of the elbow, which contributes significantly to both rotational

and varus stability of the elbow joint, is composed of the radial collateral ligament, annular ligament, lateral ulnar collateral ligament (LUCL), and accessory LUCL [9,10].

The primary goal in treating ligamentous elbow injuries is to restore the anatomy and biomechanical function of these structures. To accomplish this, a thorough understanding of the normal anatomy of the key capsuloligamentous structures as well as bony structure is necessary. Although prior investigations have evaluated the insertional footprints of the MCL and LCL complex around the elbow, the studies predominantly relied on the measurements obtained from vernier or digital caliper, which are unable to accurately measure the area of nongeometric shapes with irregular contours, such as those associated with anatomic footprints [1,11]. Several investigators developed three-dimensional (3D) anatomy using computed tomography (CT) or digitizing technology, but their methods cannot accurately define irregular areas of ligamentous attachments as well as their relationship with bony parameters such as size of the epicondyle, trochlea, and radial head [12-14].

In this study, micro-CT was used to evaluate topographic anatomy of the footprints of key ligaments of the elbow and assess their relationships with bony parameters such as the distal humerus, olecranon, and proximal ulna and radius. Previous studies utilizing micro-CT imaging techniques have demonstrated bone morphometry and microarchitecture of human bones [15-19]. We hypothesized that micro-imaging can detail the anatomy of the MCL and LCL footprint on the elbow joint and their internal microarchitecture. We also investigated the ratios of type I/III collagen at different lesions of the MCL and LCL of elbow in order to study the histological characteristics of the ligaments.

MATERIALS AND METHODS

1. Specimen preparation

Eleven human cadaver elbows (five right and sex left elbows from two males and four females; mean age at death, 76 years; range, 67–86 years) were prepared. All of the elbows had no evidence of traumatic or degenerative changes around the joint. The entire specimen was harvested from the elbow, leaving the ligaments and joint capsule intact through meticulous dissection of all periarticular skin and musculature. Each of MCL and LCL complexes was carefully cleaned of nonligamentous soft tissue and left in situ (Figs. 1, 2). We carefully examined the exact origin, insertion, and course of each ligament under microscopy (HSZ-600; HUVITZ Inc., Seoul, Korea).

Both the MCL and LCL were cut near their insertions to identify the footprints. The outlines of the footprints on the MCL and LCL were marked and painted with Telebrix (Meglumine ioxithalamate; Gubebet, Aulnay-sous-Bois, France) contrast media solution, which is commonly used for enhanced CT.

This study was approved by the Institutional Review Board of the Dankook University Hospital (No. DKUH 2016-08-016-002), and all investigations were conducted in conformity with ethical principles of research.

2. Micro-computed tomography imaging

Three-dimensional micro-CT renderings of the elbow joint were used to examine the external and internal bone architecture (SkyScan 1176; SkyScan, Antwerp, Belgium). This system

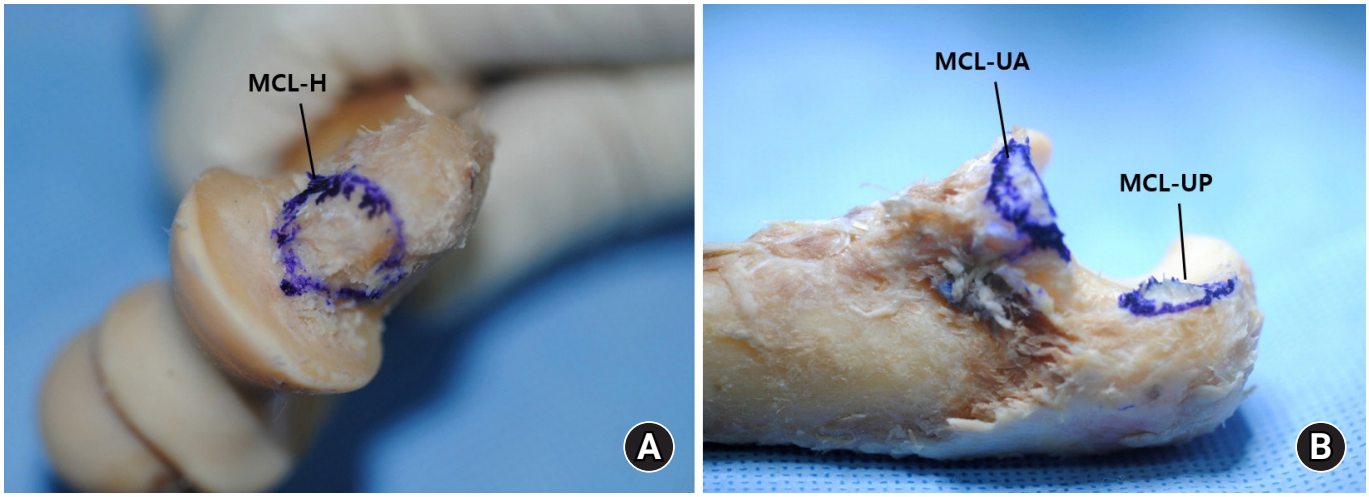

Fig. 1. The medial collateral ligament (MCL) inserting onto (A) distal humerus and (B) proximal ulna. MCL-H, humeral attachment of the MCL; MCL-UA, ulnar attachment of anterior bundle of the MCL; MCL-UP, ulnar attachment of posterior bundle of the MCL.

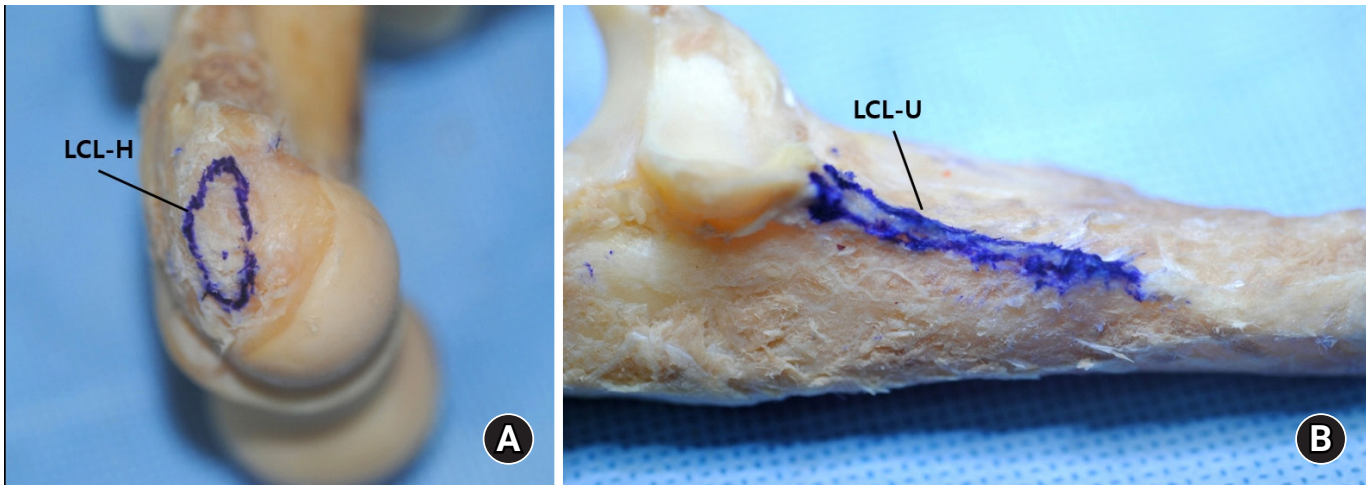

Fig. 2. The lateral collateral ligament (LCL) inserting onto (A) distal humerus and (B) proximal ulna. LCL-H, humeral attachment of the LCL; LCL-U, ulnar attachment of LCL (lateral ulnar collateral ligament, LUCL).

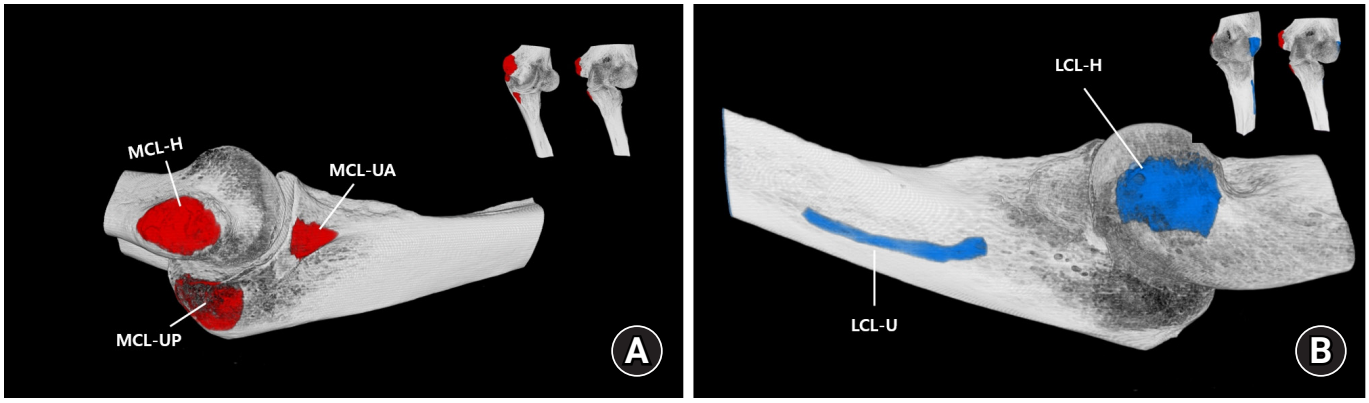

Fig. 3. A three-dimensional structural image of the elbow joint (the attachment of MCL [A] and LCL [B]; distal humerus and proximal ulna). MCL, medial collateral ligament; MCL-H, humeral attachment of the MCL; MCL-UA, anterior bundle of ulnar attachment of the MCL; MCL-UP, posterior bundle of ulnar attachment of the MCL; LCL, lateral collateral ligament; LCL-H, humeral attachment of the LCL; LCL-U, ulnar attachment of the LCL.

was comprised of an X-ray microscope with a high-definition X-ray microfocus tube, focal spot diameter of 10 μm, a 1.0 mm-thick aluminum filter to remove noise during X-ray scanning, a precision-controlled specimen holder, a two-dimensional (2D) X-ray charge-coupled device camera connected to a frame grabber, and a workstation running tomography reconstruction software (NRecon, ver. 1.6.3.3; SkyScan). A 3D structural image of the elbow joint (the attachment of MCL and LCL; distal humerus and proximal ulnar) with voxels 35×35×35 μm in size was reconstructed from 2D cross-sectional images in bitmap format with a 35-μm slice thickness (pixel, 35×35 μm).

3. Topographic parameters

After reconstructing the 3D image of the distal humerus, proximal ulna, and radius, each of the footprints of the MCL and LCL was separated from the cortical surface of the bones and reconstructed using an appropriate threshold in the software (Fig. 3) [18]. The footprint sizes, including the maximal width and length, and the area of each of their insertions were measured, using a reverse engineering software system (Rapidfom 2006; Inus Technology, Seoul, Korea). The accuracy of the area measurement was ≤0.01 mm or mm^2.

To analyze the topography of the landmarks in the elbow, coronal, sagittal, and horizontal section images were reconstructed using CT Analyzer software (DataViewer; Skyscan) (Fig. 4). The distance between medial and lateral epicondyles, width and height of the medial epicondyle, anteroposterior and mediolateral diameter of the radial head as well as height, anteroposterior and proximodistal diameters of the capitulum, anteroposterior and proximodistal diameters of the trochlea, depth of trochlea, troch-

https://doi.org/10.12790/ahm.21.0113

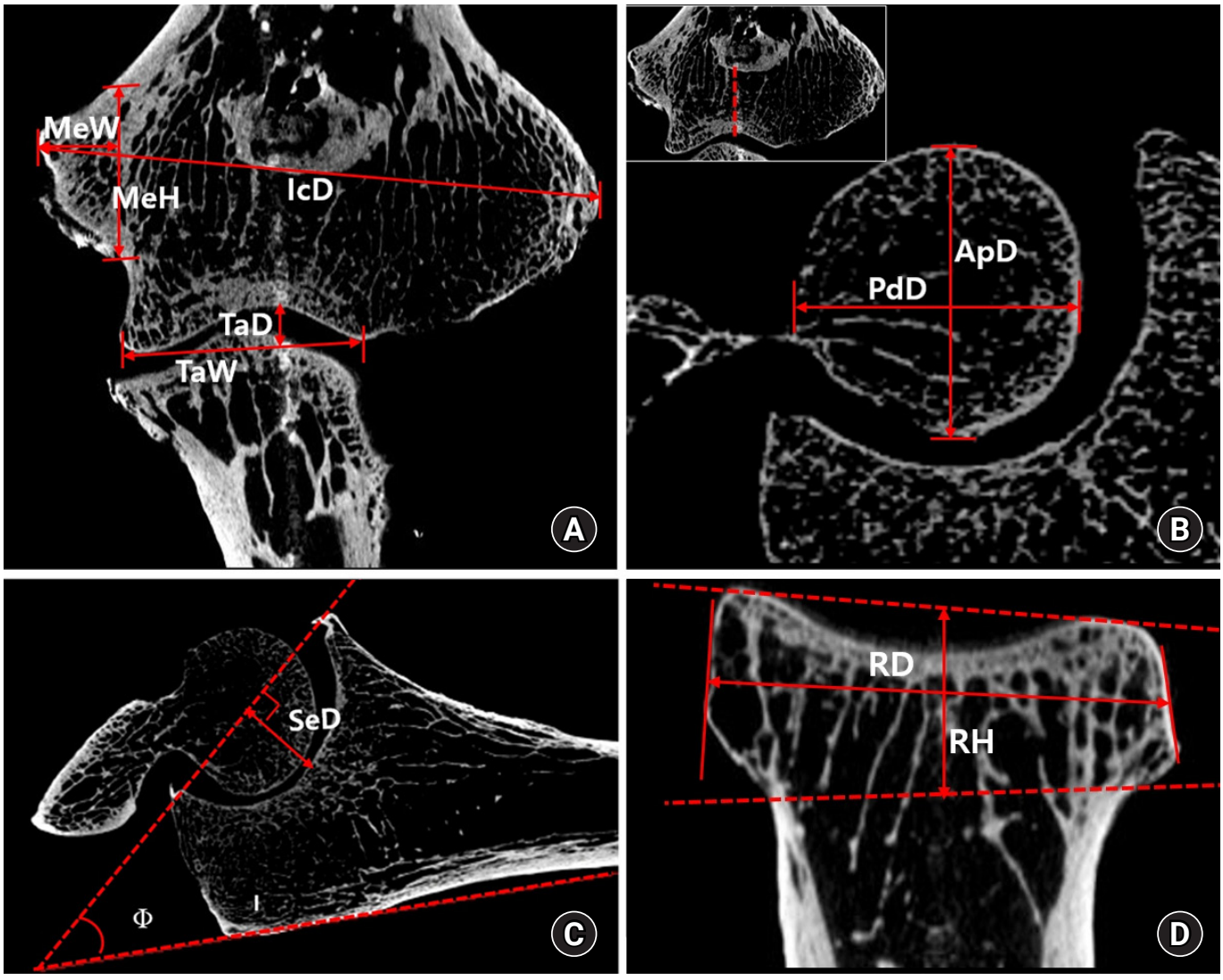

Fig. 4. Analysis of distal humerus topography on coronal and sagittal reconstructed images. (A) IcD, distance between medial and lateral epicondyles; MeW, width of the medial epicondyle; MeH, height of the medial epicondyle; TaD, depth of the trochlea; TaW, trochlea articular width. (B) ApD, anteroposterior diameter of the trochlea; PdD, proximodistal of diamter of the trochlea. (C) SeD, depth of the semilunar notch; ϕ, angle of the olecranon. (D) RD, maximal diameter of the radial head; RH, height of the radial head.

lear articular width, and depth of semilunar notch and angle of the olecranon were measured in each plane. All values were represented as mean ± standard deviation.

4. Histological characteristics of the ligaments

To compare the characteristics of collagen types between each component of the MCL and LCL, an illumination method under polarized light microscopy after picrosirius red staining was applied to 11 ligament specimens [20-22]. Five transverse sections (about 2-mm thickness) in the elbow ligaments were obtained at the mid-portion of the anterior and posterior parts of the MCL and LCL attaching near to the distal humerus as well as anterior and posterior bundles of the MCL (AB-MCL and PB-MCL, respectively) attaching to the proximal ulna. The specimens were fixed in 10% neutral buffered formaldehyde solution and embedded in paraffin. And then the specimens were stained by 0.1% picrosirius red solutions (Sirius Red F3B; Sigma-Aldrich, St. Louis, MO, USA) after sectioning along with the longitudinal direction of the fibers at 5 μm, which were similar to the previous papers [21,22]. The sections were then examined under bright field and polarizing microscopy and photographed at ×200 magnifications. Collagen fibers display uniformly as red or yellow color in type I, whereas as a greenish color in type III under polarized light. The distributions of type I/III collagen were obtained by discriminating the hue value of each pixel in the images of hue-saturation-bright-

ness color model using i-solution software (IMT i-Solution Inc., Vancouver, BC, Canada). Each of the hue values of collagen type I and III was measured in three rectangular areas (6,400 μm^2), which were randomly selected, and collagen I/III ratios were calculated (Fig. 5). Three sequential sections of each specimen were examined to reduce sampling error.

5. Statistical analysis

The results were expressed as mean ± standard deviation. A nonparametric test was used because of the small number of samples. The Friedman test was used to compare the morphometry of the footprints of the ligaments around the elbow. Repeated-measures one-way analysis of variance was performed to compare topographical parameters in medial and lateral lesions as well as collagen I/III ratios in four different lesions of the elbow ligaments. A post-hoc comparison using the Tukey correction was made if the p-value was <0.05. The Spearman correlation coefficient analysis was conducted between the topographical data of the elbow joint. A p-value of <0.05 was considered significant for all results. Analyses were performed with IBM SPSS Statistics ver. 21.0 (IBM Corp., Armonk, NY, USA).

RESULTS

1. Footprint morphometry of the medial collateral ligament and lateral collateral ligament

Location of footprints of the MCL at the humerus was inferior part of the medial epicondyle, whereas that of the LCL was posteroinferior part of the lateral epicondyle (Table 1). Areas of the MCL and LCL footprint attached to the humerus were 133.2 ± 25.8 mm^2 and 128.3 ± 23.2 mm^2, respectively, and the difference was statistically significant ($p=0.028$). The difference in circularity ratio of humeral footprint between the MCL and LCL was not significant ($p=0.972$). AB-MCL had a larger area of footprint than the PB-MCL on the ulna (mean, 109.9 ± 24.8 mm^2 vs. 89.2 ± 19.6 mm^2; $p=0.017$). The LUCL

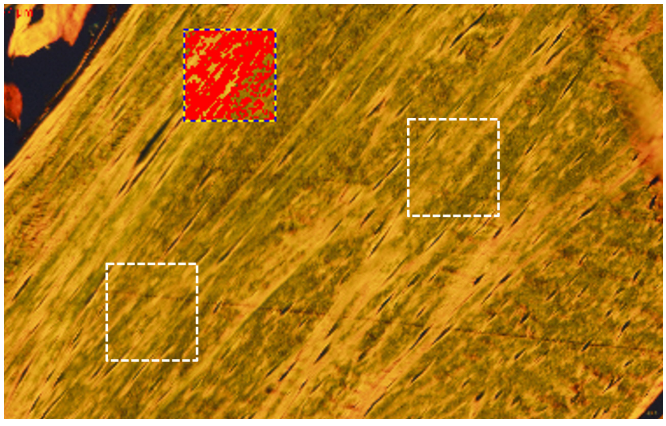

Fig. 5. The histological images of the medial collateral ligament under polarized light with picrosirius red staining (200×). Greenish birefringence was type III collagen whereas red-yellow birefringence was type I collagen. Distributions of type I/III were measured in three rectangular areas (6,400 μm²), which were randomly selected (dotted boxes).

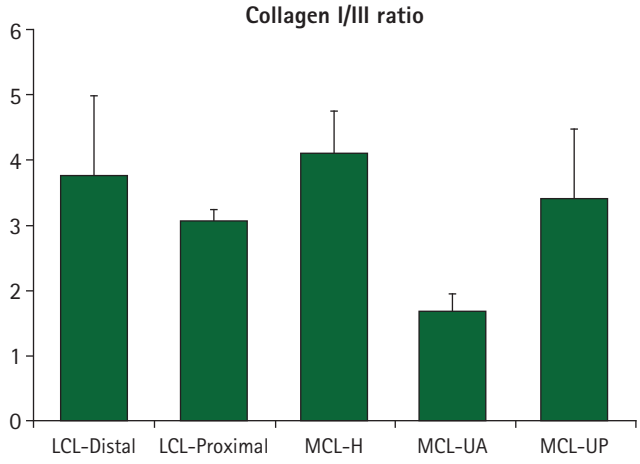

Fig. 6. Comparison of the collagen I/III ratio between the five lesions of the elbow ligaments. The error bars represented the standard deviation. LCL, lateral collateral ligament; MCL, medial collateral ligament; MCL-H, humeral attachment of the MCL; MCL-UA, ulnar attachment of anterior bundle of the MCL; MCL-UP, ulnar attachment of posterior bundle of the MCL.

Table 1. Morphometry of the footprints of the elbow ligaments

Ligament	Mean width (mm)	Mean height (mm)	Area (mm²)	Perimeter (mm)	Circularity ratio
MCL-H	12.2 ± 2.4	9.5 ± 1.75	133.2 ± 25.8	45.2 ± 5.8	1.2
MCL-UA	11.9 ± 2.7	6.5 ± 1.9	109.9 ± 24.8	42.3 ± 33.9	1.3
MCL-UP	12.3 ± 2.5	5.4 ± 1.2	89.2 ± 19.6	48.8 ± 6.7	2.1
LCL-H	14.2 ± 2.3	8.4 ± 2.0	128.3 ± 23.2	44.3 ± 5.6	1.2
LCL-U	31.7 ± 4.6	2.2 ± 0.5	89.7 ± 19.6	90.3 ± 10.5	7.2

Values are presented as mean ± standard deviation if otherwise specified.
MCL, medial collateral ligament; MCL-H, humeral attachment of the MCL; MCL-UA, ulnar attachment of anterior bundle of the MCL; MCL-UP, ulnar attachment of posterior bundle of the MCL; LCL, lateral collateral ligament; LCL-H, humeral attachment of the LCL; LCL-U, ulnar attachment of LCL.

https://doi.org/10.12790/ahm.21.0113

showed a long narrow insertion on the ulna (circularity ratio, 7.23), and the size of the footprint on the ulna was smaller than the humeral insertion (p = 0.047).

2. Topographic analysis of the elbow

The result of topographic parameters of the elbow shows in Table 2. The maximal distance between medial and lateral epicondyle averaged 52.8 ± 2.76 mm. The width and height of the medial epicondyle averaged 11.13 ± 3.33 mm and 19.25 ± 2.58 mm, respectively. The mean anteroposterior diameter of the trochlea was 18.85 ± 3.41 mm, and the size was not different compared to the diameter of the structure measured in proximal-distal direction (p = 0.001). The anteroposterior diameter of the capitulum was 18.63 ± 1.86 mm, and the size was not different from either proximal-distal diameter of the capitulum or the size of the trochlea (all comparisons, p > 0.05). Averaged semilunar notch depth and olecranon angle were 12.39 ± 2.19 mm and 27.24° ± 9.89°, respectively.

3. Correlations between the footprint parameters

The footprint area of the MCL humeral attachment was positively correlated with that of the LCL humeral attachment (r = 0.627, p = 0.039). The correlations between the footprint size of the humeral attachment and footprint size of ulnar attachment of AB-MCL and PB-MCL were not statistically significant (r < 0.475, p > 0.05). No correlation was found between footprint sizes of AB-MCL and PB-MCL, and between footprint sizes of humeral and ulnar attachments in the LCL.

4. Correlations between the footprint size and computed topographic parameters

The footprint size of the MCL humeral attachment was negatively correlated with the diameter of the radial head (r = −0.606, p = 0.048). The footprint size of the AB-MCL was positively correlated to the semilunar notch depth (r = 0.729, p = 0.017), but no correlation was observed between the other CT parameters. The footprint size of the posterior bundle of the MCL was negatively correlated with both the width and height of the medial epicondyle (r = −0.754, p = 0.012 and r = −0.681, p = 0.030, respectively).

The footprint size of the LCL humeral attachment was negatively correlated with the height of the radial head (r = −0.836, p = 0.001) and maximal diameter of the radial head (r = −0.662, p = 0.026), and positively correlated with the trochlea articular width (r = 0.624, p = 0.040).

Table 2. Topographical parameters

Parameter	Indicator	Mean parameter	95% CI
Maximal intercondylar distance (mm)	IcD	52.8 ± 2.8	48.0 ± 2.8 to 56.0 ± 2.8
Width of the medial epicondyle (mm)	MeW	11.1 ± 3.3	5.8 ± 3.3 to 15.1 ± 3.3
Height of the medial epicondyle (mm)	MeH	19.3 ± 2.6	16.1 ± 2.6 to 23.8 ± 2.6
Trochlea articular width (mm)	TaW	26.4 ± 3.4	20.4 ± 3.4 to 30.5 ± 3.4
Trochlea articular depth (mm)	TaD	6.6 ± 1.4	4.2 ± 1.4 to 8.5 ± 1.4
Anteroposterior diameter of the trochlea (mm)	ApD	18.8 ± 2.4	14.4 ± 2.4 to 22.5 ± 2.4
Proximodistal diameter of the trochlea (mm)	PdD	20.1 ± 2.9	14.0 ± 2.9 to 24.0 ± 2.9
Diameter of the radius head (mm)	RD	21.3 ± 1.1	19.3 ± 1.1 to 26.2 ± 1.1
Height of the radius head (mm)	RH	10.0 ± 1.4	7.0 ± 1.4 to 13.8 ± 1.4
Depth of the semilunar notch (mm)	SeD	12.4 ± 2.2	9.5 ± 2.2 to 16.4 ± 2.2
Angle of the olecranon (°)	ϕ	27.2 ± 9.9	14.7 ± 9.9 to 40.8 ± 9.9

Values are presented as mean ± standard deviation. CI, confidence interval.

Table 3. Comparison of the collagen I, III and I/III ratio between the five lesions of the elbow ligament

Ligament	Collagen I, green (μm²)	Collagen III, red-orange (μm²)	Collagen I/III ratio
LCL-Distal	2,164.4 ± 1,560.0	2,184.8 ± 1,086.4	3.8 ± 1.2
LCL-Proximal	1,633.3 ± 1,316.7	2,793.0 ± 858.1	3.0 ± 0.2
MCL-H	1,439.3 ± 1,249.8	2,782.7 ± 1,000.7	4.1 ± 0.6
MCL-UA	2,426.4 ± 1,302.9	2,330.4 ± 885.7	1.7 ± 0.3
MCL-UP	1,347.7 ± 1,097.3	2,502.9 ± 934.7	3.4 ± 1.1

Values are presented as mean ± standard deviation.
LCL, lateral collateral ligament; LCL-Distal, distal of humeral attachment of the LCL; LCL-Proximal, proximal of humeral attachment of the LCL; MCL, medial collateral ligament; MCL-H, humeral attachment of the MCL; MCL-UA, anterior bundle of ulnar attachment of the MCL; MCL-UP, posterior bundle of ulnar attachment of the MCL.

5. Characteristics of collagen types in the elbow ligament

The results of the collagen I/III ratios for five different sections of the elbow ligament were shown in Table 3 and Fig. 6. The collagen I/III ratio of the humeral attachment of the MCL was 4.12±0.63, which was the greatest among the five sections, and the difference was significant compared to its distal attachments.

DISCUSSION

The elbow has medial and lateral ligamentous structures that provide stability to the elbow reinforcing the anatomic congruity of the osseous anatomy. The medial collateral ligament itself consists of two parts; anterior and posterior bundle. Generally, it has been known that the anterior bundle of the MCL originates in the medial epicondyle and inserts in the sublime tubercle providing stability against valgus displacement while the posterior bundle of the MCL originates from the medial epicondyle and inserts on the olecranon and its contracture limits elbow flexion [8,23]. Dugas et al. [13] described that the morphologic characteristics of the anterior band of the MCL in 13 fresh-frozen cadaveric specimens. These authors found that footprint sizes of the MCL anterior bundle were larger than their sizes at the humeral attachment, where sizes of the humeral and ulnar attachments were 45.5 mm^2 and 127.8 mm^2, respectively. However, our study found that the footprint areas of the MCL attached to the humerus and the anterior and posterior bundles attached to the proximal ulna were 133.20 ±25.81 mm^2, 89.15±19.57 mm^2, and 109.90±24.75 mm^2, respectively. The prior investigations have evaluated the insertional footprints of the ligament based on the measurements obtained from vernier digital caliper, which are unable to accurately measure the area of nongeometric shapes with irregular contours, such as those associated with anatomic footprints [1,11]. Conversely, 3D anatomy of soft tissue reconstructed by using micro-CT like our study would provide a considerably accurate and precise measure of the complex structure [12-14].

The MCL is known to be attached to the sublime tubercle. However, Farrow et al. [24] reported a long ulnar attachment of the MCL along the medial aspect of the proximal ulna, of which structure is nominated as the MCL ridge. The authors found these osseous and ligamentous structures in all cadaveric specimens. In contrast, Fuss [6] identified a long ulnar attachment in only 1 of 20 specimens. Accordingly, we did not observe this anatomic variant which is a definitely long ulnar attachment of the MCL described by Farrow et al. [24]. Instead, we only noted the osseous ridge related to the sublime tubercle in 3D reconstruction images.

The LCL, especially LUCL, confers stability to the radiocapitellar and ulnohumeral articulations and demonstrated some variability in interindividual anatomy [1]. Most literatures have suggested that the LUCL is the most important stabilizing part of the lateral ligament complex [9,25,26]. Capo et al. [12] reported that the LUCL had a mean origin footprint of 136 mm^2 at the distal humerus and an insertional footprint of 142 mm^2 at the proximal ulna, and the sizes of LUCL footprint at the origin and insertion were 59% and 8% of footprint of the MCL, respectively. Similarly, our study demonstrated that sizes of LCL footprints were 128 mm^2 at the humeral origin. However, the LCL footprint measured at the distal ulnar insertion was 89 mm^2, which is different from the data of Capo et al. [12]. Unlike the medial side, distinct fascicles of the LCL complex cannot be clearly individualized. Despite that the LUCL usually reaches the supinator crest but also further distally onto the shaft of the ulna [6,8], the previous literature roughly measured distal insertional footprint. Furthermore, the study relied on measurements obtained from computer-assisted digitizing system which cannot accurately define irregular area of interest. Knowledge of distal long insertion of the LUCL, as seen in our study, is useful to help guide an anatomic reconstruction and therefore restore biomechanics and elbow range of motion, especially when injury to these structures makes determining accurate footprint positions challenging [13].

Although much is already known about the anatomy of the MCL and LCL, to the best of our knowledge, no prior study has demonstrated the correlation between footprint sizes of MCL and LCL and radiologic humeral parameters [12,13,23]. We found that size of MCL humeral attachment was positively correlated with that of the LCL humeral attachment, but size of both humeral footprints had a weak correlation with each size of distal insertional footprints. The fiber bundles could be seen quite differently from one another when the several parts of the collateral ligament were dissected and divided into several fiber bundles. Furthermore, some ligament fibers originated from the humerus might be combined with the capsular structure [6].

The mechanical properties of ligaments are strictly related to both collagen arrangement of type I and III and collagen fibril size, advising that collagen fiber bundle arrangement presumably differs from ligament to ligament [27-29]. An increase in the percentage of type III collagen in a healed ligament resulted in decreasing its mechanical property, whereas an increase of type I than type II collagen resulted in increasing mechanical property [27,28]. Fuss [6] described that the anterior fiber bundle of the MCL is much more closely packed than the posterior part. However, we did not find any difference in collagen I/III

https://doi.org/10.12790/ahm.21.0113

ratios between in proximal and distal parts of both the MCL and LCL. This indicates that the internal mechanical properties of the collateral ligaments were similar whether their stumps are proximal or distal and anterior or posterior. Consequently, the mechanical strength of the LCL and MCL might be determined based on the size of the ligament rather than pattern of collagen arrangement [27,29].

The MCL is the primary stabilizer to valgus moment, whereas the radial head contributes minimally to valgus stress [8,30]. Our hypothesis for the findings of present study which showed a negative correlation between the footprint size of the MCL at humeral side and size of the radial head would be that strong constraint due to thick MCL does not require a large radial head. In addition, the footprint size of the AB-MCL was positively correlated with the semilunar notch depth. Because little has been published on the correlation between anatomy of the MCL and radiologic parameters, we could not prove this finding. However, it's our assumption that the deeper semilunar notch requires the larger area of soft tissue coverage which might be critical for resisting valgus moment [30].

There are several limitations to this study. First, this study had a small number of specimens. However, the consistency of distinct footprint patterns of the LUCL and MCL in all specimens indicates that our description is reliable. Second, this study was not based on the elbow parameters measured in simple radiography, which may be limitedly applied to clinical perspectives. Third, this study was less clearly visualization of the footprints by painting them with contrast media on the lesion of interest. Fourth, this study included some old-aged specimens. Because degenerative change around the elbow might lead to deformation of topographic morphometry of the footprint, our data might skew the statistics. Finally, the measurement of the distribution of collagen type I/III ratio was dependent upon observer factors, such as how much the hue value of each pixel was discriminated in the images.

CONCLUSION

This study demonstrated that the topographic anatomy of the attachment of the LUCL and MCL providing primary varus and valgus stability of the elbow and assessed their relationships with bony parameters. There was a negative correlation between the footprint size of the MCL at humeral side and size of the radial head as well as a positive correlation between the footprint size of the AB-MCL and the semilunar notch depth. A better understanding of the MCL and LCL and their relationship with osseous anatomy will assist with anatomic reconstruction of the ligaments.

CONFLICTS OF INTEREST

The authors have nothing to disclose.

REFERENCES

1. Reichel LM, Morales OA. Gross anatomy of the elbow capsule: a cadaveric study. J Hand Surg Am. 2013;38:110-6.
2. Dodson CC, Thomas A, Dines JS, Nho SJ, Williams RJ 3rd, Altchek DW. Medial ulnar collateral ligament reconstruction of the elbow in throwing athletes. Am J Sports Med. 2006;34:1926-32.
3. Paletta GA Jr, Wright RW. The modified docking procedure for elbow ulnar collateral ligament reconstruction: 2-year follow-up in elite throwers. Am J Sports Med. 2006;34:1594-8.
4. Rohrbough JT, Altchek DW, Hyman J, Williams RJ 3rd, Botts JD. Medial collateral ligament reconstruction of the elbow using the docking technique. Am J Sports Med. 2002;30:541-8.
5. Thompson WH, Jobe FW, Yocum LA, Pink MM. Ulnar collateral ligament reconstruction in athletes: muscle-splitting approach without transposition of the ulnar nerve. J Shoulder Elbow Surg. 2001;10:152-7.
6. Fuss FK. The ulnar collateral ligament of the human elbow joint. Anatomy, function and biomechanics. J Anat. 1991;175:203-12.
7. Williams PL, Warwick R. Gray's anatomy. 36th ed. Edinburgh: Churchill Livingsone; 1980.
8. Morrey BF, An KN. Articular and ligamentous contributions to the stability of the elbow joint. Am J Sports Med. 1983;11:315-9.
9. O'Driscoll SW, Bell DF, Morrey BF. Posterolateral rotatory instability of the elbow. J Bone Joint Surg Am. 1991;73:440-6.
10. Olsen BS, Vaesel MT, Søjbjerg JO, Helmig P, Sneppen O. Lateral collateral ligament of the elbow joint: anatomy and kinematics. J Shoulder Elbow Surg. 1996;5(2 Pt 1):103-12.
11. Jarrett CD, Weir DM, Stuffmann ES, Jain S, Miller MC, Schmidt CC. Anatomic and biomechanical analysis of the short and long head components of the distal biceps tendon. J Shoulder Elbow Surg. 2012;21:942-8.
12. Capo JT, Collins C, Beutel BG, et al. Three-dimensional analysis of elbow soft tissue footprints and anatomy. J Shoulder Elbow Surg. 2014;23:1618-23.
13. Dugas JR, Ostrander RV, Cain EL, Kingsley D, Andrews JR. Anatomy of the anterior bundle of the ulnar collateral ligament. J Shoulder Elbow Surg. 2007;16:657-60.

14. Miyake J, Oka K, Moritomo H, Sugamoto K, Yoshikawa H, Murase T. Open reduction and 3-dimensional ulnar osteotomy for chronic radial head dislocation using a computer-generated template: case report. J Hand Surg Am. 2012;37:517-22.
15. Hsu JT, Chen YJ, Ho JT, et al. A comparison of micro-CT and dental CT in assessing cortical bone morphology and trabecular bone microarchitecture. PLoS One. 2014;9:e107545.
16. Hsu JT, Wang SP, Huang HL, Chen YJ, Wu J, Tsai MT. The assessment of trabecular bone parameters and cortical bone strength: a comparison of micro-CT and dental cone-beam CT. J Biomech. 2013;46:2611-8.
17. Jenkins PJ, Ramaesh R, Pankaj P, et al. A micro-architectural evaluation of osteoporotic human femoral heads to guide implant placement in proximal femoral fractures. Acta Orthop. 2013;84:453-9.
18. Norman DG, Getgood A, Thornby J, et al. Quantitative topographic anatomy of the femoral ACL footprint: a micro-CT analysis. Med Biol Eng Comput. 2014;52:985-95.
19. Rozental TD, Deschamps LN, Taylor A, et al. Premenopausal women with a distal radial fracture have deteriorated trabecular bone density and morphology compared with controls without a fracture. J Bone Joint Surg Am. 2013;95:633-42.
20. Cohen DB, Kawamura S, Ehteshami JR, Rodeo SA. Indomethacin and celecoxib impair rotator cuff tendon-to-bone healing. Am J Sports Med. 2006;34:362-9.
21. Junqueira LC, Bignolas G, Brentani RR. Picrosirius staining plus polarization microscopy, a specific method for collagen detection in tissue sections. Histochem J. 1979;11:447-55.
22. Wan C, Hao Z, Wen S. A quantitative comparison of morphological and histological characteristics of collagen in the rabbit medial collateral ligament. Ann Anat. 2013;195:562-9.
23. Barco R, Antuña SA. Management of elbow trauma: anatomy and exposures. Hand Clin. 2015;31:509-19.
24. Farrow LD, Mahoney AJ, Stefancin JJ, Taljanovic MS, Sheppard JE, Schickendantz MS. Quantitative analysis of the medial ulnar collateral ligament ulnar footprint and its relationship to the ulnar sublime tubercle. Am J Sports Med. 2011;39:1936-41.
25. O'Driscoll SW, Morrey BF, Korinek SL, An KN. Elbow joint instability: A kinematic model. J Shoulder Elbow Surg. 1994;3:143–50.
26. O'Driscoll SW, Morrey BF, Korinek S, An KN. Elbow subluxation and dislocation. A spectrum of instability. Clin Orthop Relat Res. 1992;(280):186-97.
27. Hart RT, Hennebel VV, Thongpreda N, Van Buskirk WC, Anderson RC. Modeling the biomechanics of the mandible: a three-dimensional finite element study. J Biomech. 1992;25:261-86.
28. Liu SH, Osti L, Henry M, Bocchi L. The diagnosis of acute complete tears of the anterior cruciate ligament. Comparison of MRI, arthrometry and clinical examination. J Bone Joint Surg Br. 1995;77:586-8.
29. Parry DA, Barnes GR, Craig AS. A comparison of the size distribution of collagen fibrils in connective tissues as a function of age and a possible relation between fibril size distribution and mechanical properties. Proc R Soc Lond B Biol Sci. 1978;203:305-21.
30. Cage DJ, Abrams RA, Callahan JJ, Botte MJ. Soft tissue attachments of the ulnar coronoid process. An anatomic study with radiographic correlation. Clin Orthop Relat Res. 1995;(320):154-8.

https://doi.org/10.12790/ahm.21.0113